

NONLINEAR DYNAMICS OF ROCK: HYSTERETIC BEHAVIOR

L. A. Ostrovsky^{1,2} and P. A. Johnson³

We discuss the dynamics of media with hysteretic stress–strain properties. First, experimental evidence of the hysteretic behavior of rock is presented. This evidence leads to a pattern of unifying behavior whose origin is within the “bond system” of the material, which includes small cracks, intergrain contacts and, the cement that holds the grains in place. Nonlinear response is evident over a large frequency interval (dc to several MHz at least), and it is significant from strains of plasticity down to the smallest measurable strains (order $10^{-8} - 10^{-9}$). Second, some models related to such a behavior are outlined. Finally, oscillations and waves in hysteretic media are discussed.

1. INTRODUCTION

The famous book “Oscillation theory” by Andronov, Witt, and Khaikin [1] provides a clear idea of phase plane, limit cycle, and, finally, hysteresis as a multivalued response of a system to a forcing dependent on the history of the process. Topologically speaking, these notions are associated with some closed figures, loops, on the plane of the dynamic parameters (phase plane) or that of the material parameters (hysteretic equation of state, EOS). Although the hysteretic behavior of ferromagnetics and ferroelectrics and their mechanical analogues has been studied by physicists for decades, little has been addressed regarding the theory of waves in such media except for some specific problems such as electromagnetic shock waves (e.g., [2]). It has long been known that metals can have a hysteretic mechanical EOS which in the simplest form is a dependence between the stress σ and strain ε .

Beginning in the 1940’s, Birch’s group at Harvard University began the study of the static nonlinear properties of rock. These studies, conducted in large mechanical presses, were designed to interrogate the EOS in rock samples at strong, low frequency forcing (near dc). Static tests were aimed at understanding the nature of the earth’s interior in terms of pressure and temperature response and to predict mineral assemblages and their phases in the earth’s lower crust and mantle. These studies have been invaluable in understanding and modeling physical properties and inferring the composition of the earth’s interior. In the early 1970’s, Stacy’s group at the University of Queensland wrote a series of papers on mechanical hysteresis in rocks at low strains. Their work showed that nonlinear response persists in quasistatic tests at strains as low as 10^{-6} , and perhaps lower. In the early 1980’s, Bakulin and Protosenya and a group at the Radiophysical Institute and the Institute of Applied Physics in Nizhny Novgorod began studies of nonlinear response in earth materials.

As early as 1986, there was an international symposium on nonlinear seismology organized by the Moscow Earth Physics Institute, held in Suzdal, USSR, and soon thereafter, a special issue of *Physics of the Earth and Planetary Interiors* (V. 50, No.1, 1987) devoted to nonlinear seismology appeared.

¹ Zel Technology / NOAA Environmental Technology Laboratory, Boulder, Colorado, USA; ² Institute of Applied Physics of the Russian Academy of Sciences, Nizhny Novgorod, Russia; ³ Los Alamos National Laboratory, Los Alamos, New Mexico, USA. Translated from *Izvestiya Vysshikh Uchebnykh Zavedenii, Radiofizika*, Vol. 44, Nos. 5–6, pp. 487–501, May–June, 2001. Original article submitted March 22, 2001.

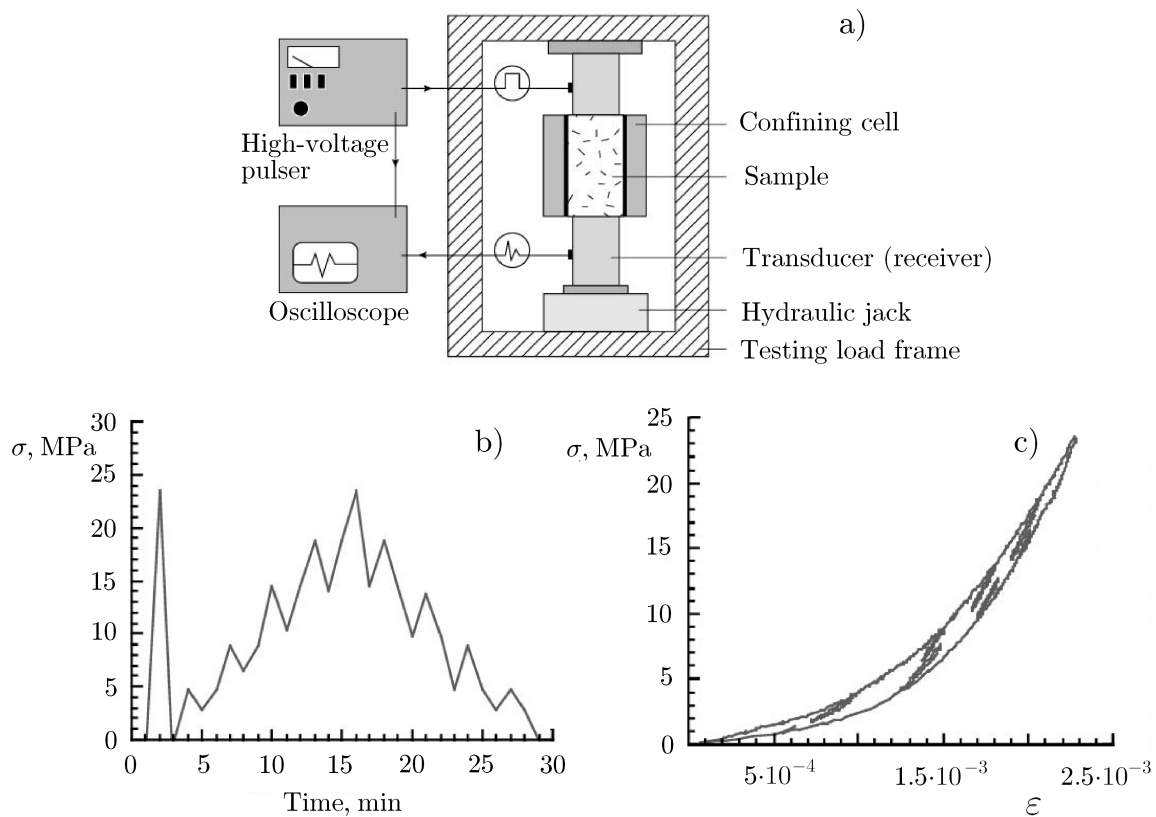


Fig. 1. Static stress–strain experiment: Typical experimental configuration for a uniaxial stress (a). Stress history or “protocol” (b). Resulting stress–strain dependence for sandstone (c). The plot illustrates a nonlinear stress–strain relation, hysteresis, and end-point (discrete) memory.

Studies of mechanical hysteresis in the EOS began to accelerate when our groups at the Institute of Applied Physics and the Los Alamos National Laboratory began to actively investigate dynamical (vibrational, acoustical) properties in earth materials. Most attention in our recent research has been paid to rock. The cumulative results of these studies confirmed that rock nonlinearity is very strong compared to that of “normal” media like fluids and ideal crystals, and the nonlinearity reveals itself even at extremely small, “acoustical” strain amplitudes. Relevant to that, in 1996–1999, the first four International Workshops on Nonlinear Mesoscopic Elasticity were held at the Institute of Geophysics and Planetary Physics at Los Alamos National Laboratory. Here, we outline some facts and ideas; an interested reader can find additional material and detailed references in the illustrative paper [3] and a detailed review [4].

2. SOME EXPERIMENTAL INDICATORS OF HYSTERETIC NONLINEARITY IN ROCKS

Dynamic nonlinear response may manifest itself in a variety of manners. Let us outline some key indicators of nonlinear hysteretic behavior of rock from the static and, mostly, dynamic data of laboratory experiments.

2.1. Quasi-static experiments

The most direct observation of elastic nonlinearity in solids comes from quasi-static tests of stress versus strain. Figure 1 shows experimental results illustrating such a dependence [5]. Primary characteristics illustrated by such an experiment are: (1) extreme nonlinearity in the stress–strain dependence, (2) hysteresis (i.e., behavior depending on stress history) and, (3) “discrete memory” (also called “end point memory”). Discrete memory can be described as follows. If a partial stress cycle is conducted during the quasistatic

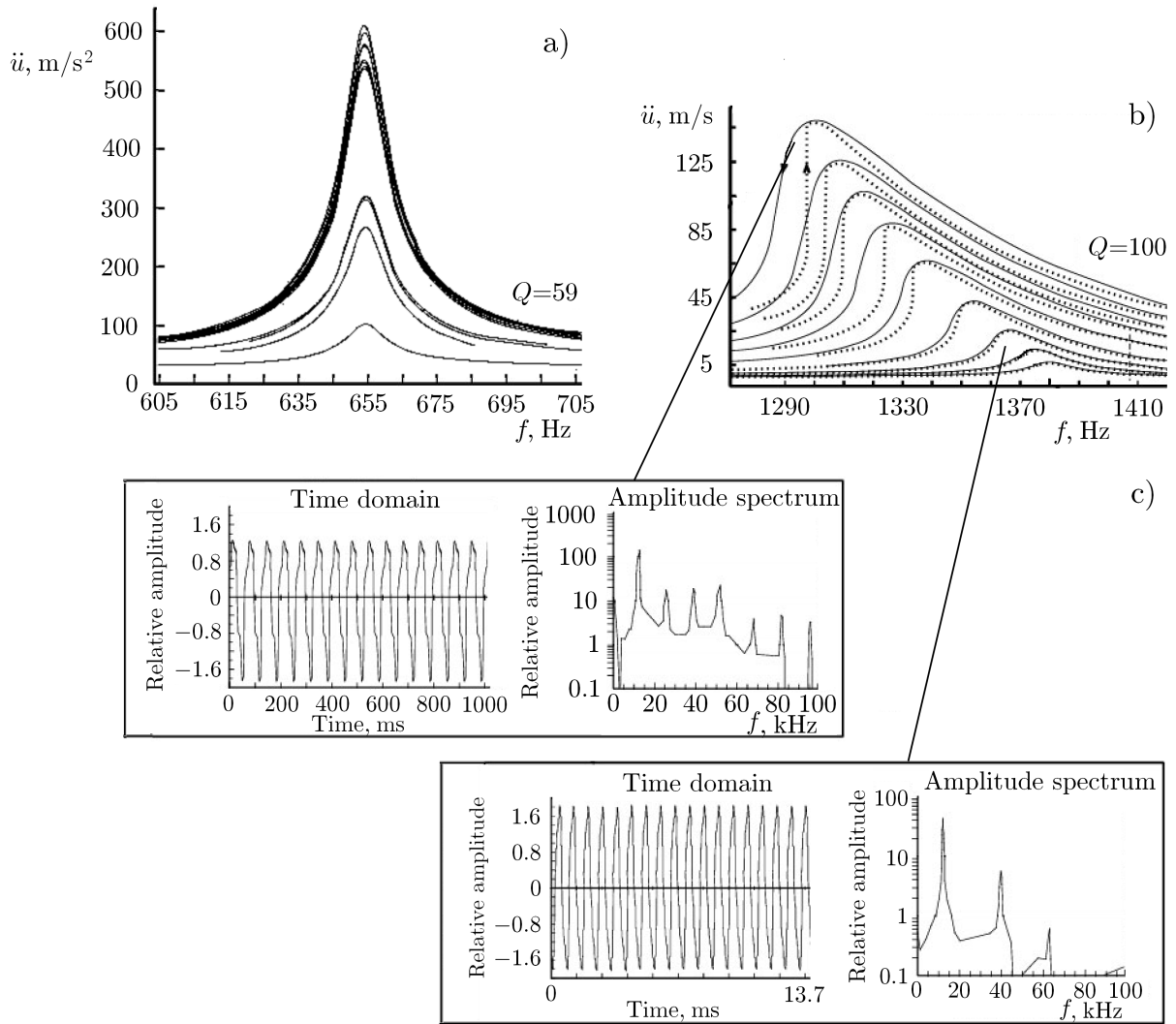


Fig. 2. Resonance acceleration response of polyvinylchloride (PVC) for several drive levels (a). Resonance acceleration response of a Fontainebleau sandstone bar, for increasing drive (b). Time and frequency domain signals from relatively low-amplitude (albeit already nonlinear) drive levels (bottom), and at large drive levels (top) (c). The time signals are obtained at peak resonances in each case, Q is the quality factor of a sample, and $f = \omega/2\pi$.

cycle (e.g., small loops inside the big loop in Fig. 1c), the outer (low frequency) loop is maintained; discrete memory is a memory of the previous maximum strain state. Similar results have been obtained by numerous other researchers since the 1970s (e.g., [6, 7]).

These manifestations have important consequences for the elastic modulus of the material defined as the derivative of the stress over the strain, $\partial\sigma/\partial\varepsilon$. In short, static tests indicate that the value of the modulus depends on the stress history and the current EOS amplitudes, and changes discontinuously at the stress-strain cusps.

2.2. Dynamic experiments

There exist numerous methods by which to observe dynamic nonlinear effects. In the ultrasonic range typically used in the acoustics of liquids and gases, the harmonics of a periodic travelling wave can be monitored out to the distance of shock wave formation. However, for relatively low-frequency and low-amplitude sound in solids, it is often difficult to obtain quantitative results from travelling wave experiments.

The majority of quantitative measurements for rocks have been performed with resonant bars. Due to the amplification that resonance provides, it is perhaps the most sensitive manner by which to observe nonlinear behavior, even at extremely small exciting strains, even at $\varepsilon = 10^{-9}$ in a simple one-dimensional configuration $\varepsilon = \partial u / \partial x$, where u is the displacement.

The corresponding dynamic experiments in solids are based on the relation between the detected strain amplitude at the drive frequency and, typically, the following: (1) harmonic amplitudes, (2) wave cross-modulation amplitudes, (3) resonance frequency shift, and (4) amplitude dependent losses. It is the observation of these effects that tell us about the nature of the nonlinearity, for instance, whether or not nonclassical behavior such as hysteresis is present in dynamic processes.

2.3. Nonlinear resonance frequency shift

The dependence of a mode resonance frequency in a sample on the oscillation amplitude is a sensitive measure that can be used for calculation of the average modulus and wave speed in rock.

Nonlinear resonance in a classical system is due to cubic nonlinearity (or its equivalent) and can be attributed to the Duffing-type equation

$$\ddot{u} + \omega_0^2 (u + pu^3) + g \dot{u} = F_0 \cos(\omega t), \quad (1)$$

where p defines nonlinearity and g , dissipation. It is well known that the resonance response of such an oscillator to the force amplitude F_0 is such that (for small g) the amplitude maximum is shifted from the linear resonance frequency ω_0 at a value of $\Delta\omega$ proportional to F_0^2 . This result is rather universal for all systems when the equation of state can be represented as a polynomial.

Let us look now at the experimental results. Figure 2a shows resonances in a “classical” medium (polyvinylchloride) at different amplitudes; it is typical of the linear behavior. Figure 2b is representative for nonlinear resonant behavior in a rock observed in Los Alamos [8]. The material is Fontainebleau sandstone under ambient temperature and pressure conditions. The solid and dotted lines in Fig. 2b indicate that the resonance response is dependent on the direction of the frequency shift (up or down the frequency axis). Clearly, the intensity of the distortion increases significantly with wave amplitude. Some relevant wave forms and signal spectra are shown in Fig. 2c.

Figure 3 illustrates the dependence between the detected frequency shift and the strain for different rocks. In all cases, this dependence is close to linear rather than to quadratic. This is unexpected behavior for classical nonlinear elasticity, where the dependence is quadratic, and implies that the equation of state contains singularities. More specifically, hysteresis is present. Note also that the nonlinearity is well measurable at strains as small as $10^{-8} - 10^{-7}$, and that strain is actually equivalent to the acoustic Mach number!

A complementary series of experiments was performed at the Institute of Applied Physics [9]. The measurements were performed in samples of granite and for a cylinder filled with wet sand; the latter was pre-consolidated by exposing it to intense sound over 4 hours to obtain stable results. Figure 4 shows the resonance frequency shift for these materials as a function of strain amplitude ε_0 . As with the data shown in Fig. 3, the shift is linearly proportional to ε_0 for the granite and the sand. Of significance is that these

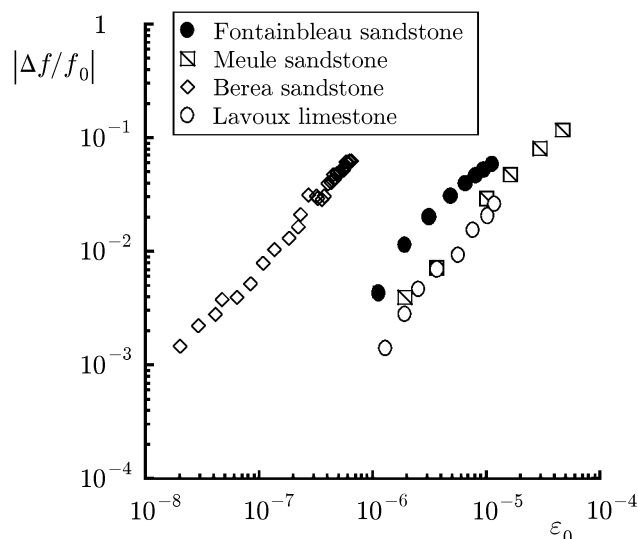


Fig. 3. Normalized frequency shift $|f - f_0|/f_0$, where f_0 is the linear resonance peak, versus strain amplitude ε_1 for various rocks under various experimental conditions. A slope of approximately 1 indicates that nonclassical nonlinearity is responsible for the peak shift.

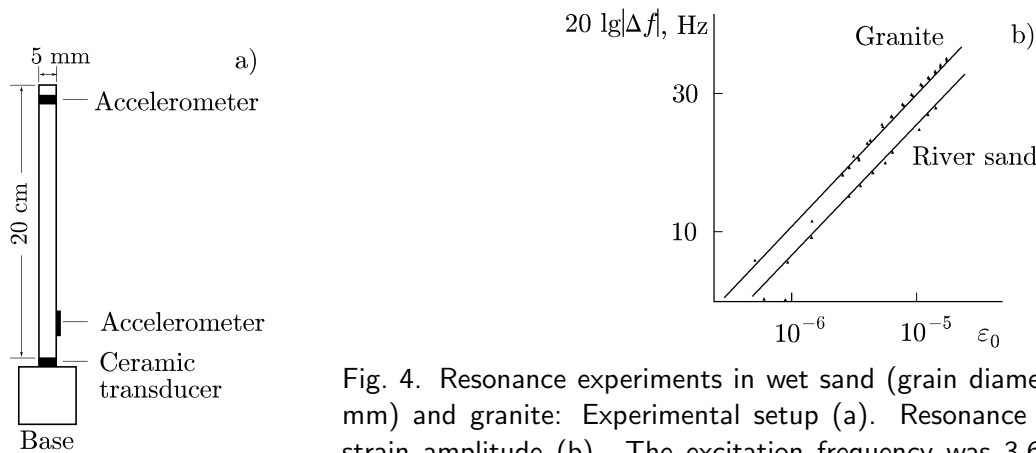


Fig. 4. Resonance experiments in wet sand (grain diameters of about 0.3 mm) and granite: Experimental setup (a). Resonance peak shift versus strain amplitude (b). The excitation frequency was 3.6 kHz (first-mode resonance) and $\Delta f = f - f_0$.

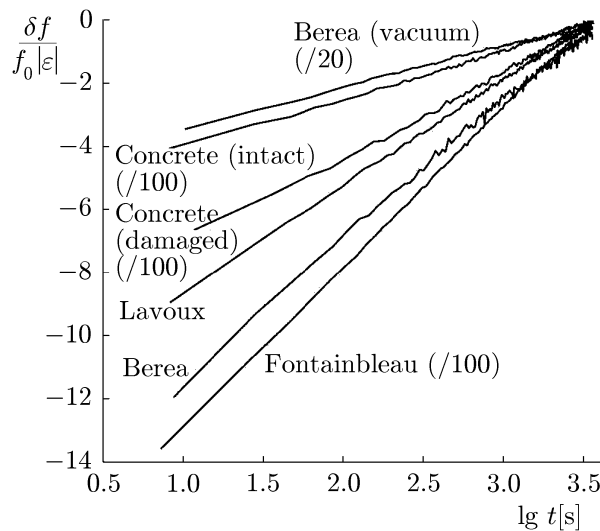


Fig. 5. Slow dynamical response in several rock types and in concrete. The time-dependent shift δf of the recovering resonant frequency, normalized to the asymptotic value f_0 , per unit driving strain $|\varepsilon|$. Sample names are indicated in the figure, and some data were divided by the indicated factors for plotting convenience. Lavoux is a limestone, Berea and Fontainebleau are sandstones, and one sample of concrete was damaged.

2.4. Harmonic generation

A large series of resonance experiments dealt with measurement of harmonic amplitudes via Fourier analysis. For instance, a typical result for Berea sandstone taken from [8] is shown in Fig. 6a. The fact that the second and third harmonic amplitude slopes are both proportional to the square of the driving force amplitude also indicates that classical nonlinearity is not sufficient to explain such behavior. Indeed, a classical stress-strain relation, like Eq. (2) below, always provides a cubic dependence of the third harmonic amplitude on the main one.

The corresponding dependences obtained in other experiments [9] are shown in Figs. 6b and 6c for granite and wet sand. These results further indicate that the EOS does not correspond to classic nonlinearity and should be singular.

are some of the very few existing measurements in unconsolidated material, the sand, and they show the same dependence with strain as the rocks. However, a different dependence was found in marble.

It is notable that the rock samples demonstrate slow dynamical (relaxation) response. Slow dynamics in this context means that the average material modulus is temporarily altered (lowered) during wave excitation. After wave excitation, it takes some time (of the order of 10^3 s) for the modulus of the material to recover its original state. One manner in which to observe this behavior is to monitor the resonance frequency before and after large excitation (e.g., [10, 11]). That is, after measuring the linear resonant peak, the sample is driven at a large amplitude for several minutes. The low-amplitude resonance is then monitored until the resonant peak has returned to its original frequency. An example of slow dynamics is illustrated in Fig. 5 for several different rock types and for concrete. It is interesting that the resonance frequency recovery is universally logarithmic in time. All this is further demonstration of the nonclassical behavior of materials.

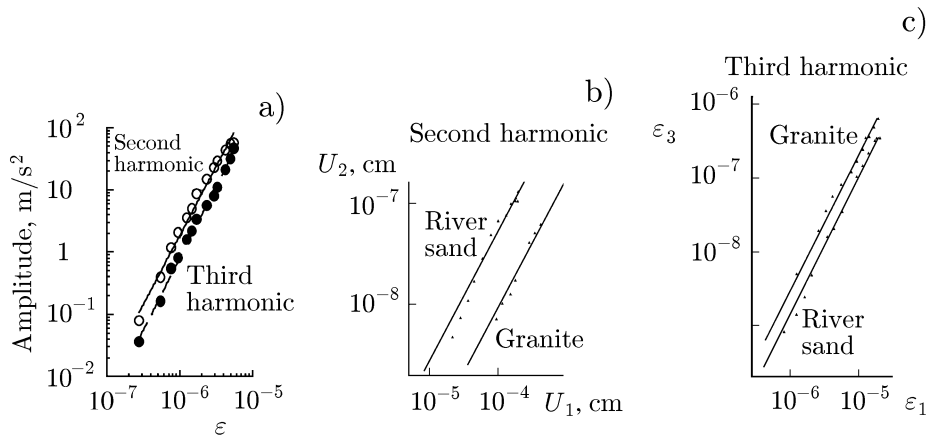


Fig. 6. Second- and third-harmonic amplitudes at resonance peaks as functions of the measured strain amplitude in Berea sandstone (a). Displacement amplitude of the second harmonic U_2 versus the fundamental displacement amplitude U_1 in river sand and granite (b). Amplitude ε_3 of the third harmonic of strain versus fundamental strain amplitude ε_1 in these materials (c). The fits correspond to a power law of 2, indicating nonclassical nonlinearity.

2.5. Nonlinear dissipation

Amplitude-dependent loss is a well-known phenomenon in metals where it is attributed to hysteresis due to dislocations. For rocks, for soils, and in earthquake studies (e.g., [12]) nonlinear dissipation is nearly always observed and is an additional indicator of hysteresis in the EOS. Below, we give two examples.

Amplitude-dependent attenuation in earth materials was observed in experiments on the nonlinear interaction between low- and high-frequency signals [13, 14]. During the low-frequency, high-amplitude resonant excitation (“pump wave”), a longitudinal ultrasound pulse (frequency 200 kHz, pulse duration 70 ms) was generated to propagate for some distance along the bar, after which its amplitude was measured, and the spatial damping rate was calculated. In the presence of the low-frequency mode, the ultrasound damping rate increased in proportion to the low-frequency strain amplitude ε_1 in granite and sand, and to ε_1^2 in marble (Fig. 7). Similar experiments for control samples (glass) did not reveal any significant nonlinear effects.

Figures 7b and 7c show results from a resonance experiment in Berea sandstone [15] under vacuum conditions at very small acceleration/strain levels. In the resonance data shown in Fig. 7b, a very small frequency shift and peak broadening can be observed. Figure 7c shows the actual change in the sample quality factor extracted from Fig. 7b. It is remarkable that nonlinear attenuation can occur at extremely small strain levels when the nonlinear frequency shift is not clearly noticeable yet.

3. MODELS OF STRUCTURAL NONLINEARITY

An adequate physical model of rock must be associated with their complex structure. The mechanical properties of rock appear to be a part of a broader class of materials, one we call the “Structural Nonlinear Elasticity” class (also “Mesoscopic/Nanoscale Elasticity”). These terms are in contrast to materials that display classical, “atomic” elasticity, such as most fluids and monocrystalline solids. The nonlinearity of atomic elastic materials is due to the atomic/molecular lattice anharmonicity. The latter is relatively small because the intermolecular forces are extremely strong. In contrast, the materials considered below contain small soft features that we term the “bond system” (cracks, grain contacts, dislocations, etc.) occupying a small total volume (of up to nanoscale sizes) within a hard matrix (grains, crystals) but subject to strong deformation and is the origin of strong nonlinearity, whereas the hard phase is relatively insensitive to deformation (e.g., [16, 17]).

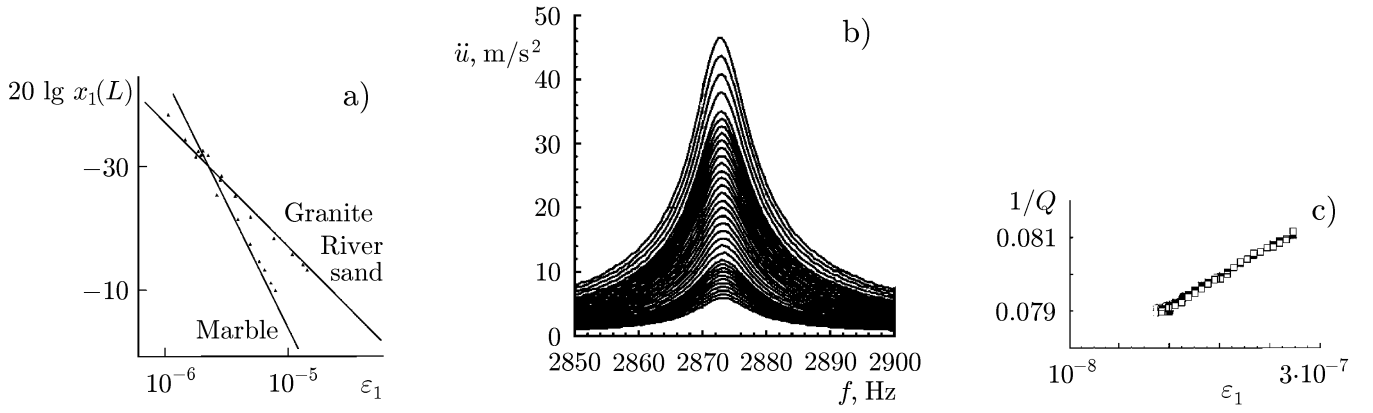


Fig. 7. Dependence of the damping rate of a 200 kHz ultrasound pulse ($X_1(L) = \ln[A_0/A(L)]$, where A_0 is the input amplitude of the pulse and $A(L)$ is output amplitude in the rod), on the amplitude ε_1 (logarithmic scale) of the low-frequency resonance “pumping” wave for three materials, obtained from the experimental configuration shown in Fig.4. For sand and granite, the dependence is linear and for the marble, quadratic (a). Resonance acceleration amplitude versus frequency at very small acceleration levels (b). From the data in (b): normalized attenuation rate $1/Q$ versus strain (logarithmic scale) (c).

An effect of the soft/hard system is well known for liquids with bubbles where the maximum nonlinearity is observed for a gas volume fraction of less than 10^{-3} (e.g., [18]). A similar behavior is demonstrated by waterlike porous media in which the shear modulus is small compared to the bulk modulus (i.e., the shear wave velocity is much smaller than that of longitudinal waves). In such cases, the parameter of nonlinearity β may reach values of $10^4 - 10^5$ compared to 1 to 10 for “classical” gases, liquids, and solids. However, no hysteresis exists in these systems.

From the above measurements one can calculate a set of fundamental nonlinear parameters of the material and use them to infer the nature of the nonlinear response and to create models.

The classical nonlinear theory for atomic elasticity is thoroughly described in literature (see [19]). It begins with the expansion of the elastic strain energy, E , in powers of the components of strain tensor, ε_{ij} . The expansion coefficients designate the components of the second-order elastic tensor and the third-order elastic tensor, respectively. These tensors are characterized, respectively, by 21 and 56 independent components for an arbitrary anisotropic medium (in the lowest-order, triclinic material symmetry) and only by 2 and, respectively, 3 components in the highest-order symmetry (isotropic material). The result is an equation of state relating the stress tensor σ_{ik} to the strain tensor. To gain an insight, one can consider the one-dimensional case. For a longitudinal wave (P -wave) propagating in an isotropic medium, a one-dimensional wave can exist with only nonzero components $\sigma_{xx} = \sigma$ and $u_x = u$ or $\varepsilon_{xx} = \varepsilon = \partial u / \partial x$. Then,

$$\sigma = M (\varepsilon + \beta \varepsilon^2 + \delta \varepsilon^3 + \dots), \quad (2)$$

where M is the elastic modulus, and β and δ are nonlinear coefficients that can be expressed in terms of combinations of the elastic moduli. A typical order of linear moduli for atomic elastic solids is $10^{11} - 10^{12}$ Pa. From here, it easily follows that the amplitude of the second harmonic of a signal, A_2 , is proportional to the square of the amplitude of the applied force, A_0 , and the third harmonic is proportional to A_0^3 .

Nonlinear response in hysteretic materials should contain an additional, singular term in EOS that is sensitive to the history of the process. The latter can be characterized by the sign of $\dot{\varepsilon} = \partial \varepsilon / \partial t$:

$$\sigma = M (\varepsilon + \beta \varepsilon^2 + \delta \varepsilon^3 + \dots) + \hat{A} [\varepsilon, \text{sign}(\dot{\varepsilon})], \quad (3)$$

where \hat{A} is a functional describing “nonclassical” effects. A specific form of \hat{A} should follow from the physics of the material. In an early work by Asano [20], two basic types of nonclassical (hysteretic in stress–strain)

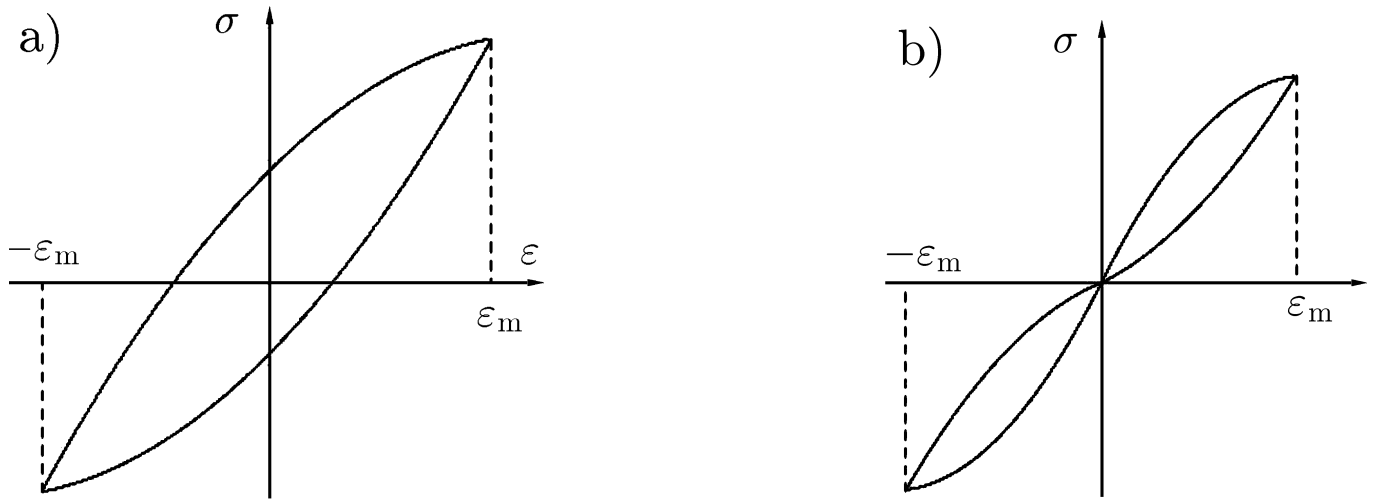


Fig. 8. Simplified forms of two hysteretic models of the EOS: irreversible (type 1) hysteresis (a) and reversible (type 2) hysteresis (b).

behavior were considered. One of them (type 1) surrounds the zero point on the (σ, ε) plane for periodic motion (Fig. 8a). The second (type 2) includes the zero point and has a “butterfly” shape (Fig. 8b); it is related to the Granato–Lücke model discussed below. Note that Asano associates them with two simple mechanical models, “slider” for type 1 and “ratchet” for type 2 which could help to understand their physical nature. In many cases, these forms were introduced as a best fit for experimental values and dependences. For example, using a specific phenomenological EOS enabled the authors of [14] to consistently describe the results of their experiments.

A semi-phenomenological model called the Preisach–Mayergoyz space (P–M space) model, which successfully describes the hysteretic nonlinear behavior of rock elasticity with discrete memory, was developed in a series of papers by our colleagues (see [3, 21] and references therein). The model assumes that the elastic properties of a macroscopic sample of material result from the integral response of a large number of individual, elastic elements (of order 10^{12} , a rough estimate of the number of grain-to-grain contacts, microcracks, etc., in one cubic centimeter of rock). Each elastic element may or may not demonstrate hysteretic behavior. The individual elements are combined for analysis in what is known as P–M space (also referred to as Preisach space). To obtain an equation of state, it is assumed that most of the elements are nonhysteretic (with weak nonlinearity). As a result, the stress–strain relation of type 2 hysteresis follows. The P–M space model gives some idea of the composition of a hysteretic media (note that the dislocations considered below can serve as its elements). However, it still remains a phenomenological description that does not contain the physical mechanisms of nonlinear response. In the following discussion, several relatively simple physical models will be tested here to see if they can provide some insight into the mechanism of nonlinear response.

3.1. Hertzian contacts

A starting point model of nonlinearity in rock can be based on representing the rock as a system of dry, contacting grains as shown in Fig. 9. These contacts are much softer than the matrix material, the grains themselves, and therefore play the primary role in the nonlinear elastic response of the medium. In this model, the distance change Δ between the grain centers is related to the compressing force, F , by the Hertzian contact law (e.g., [19])

$$\Delta = \left[\frac{3(1 - \nu^2)F}{4ER^{1/2}} \right]^{2/3}, \quad (4)$$

where E is the Young’s modulus of the material, ν is the Poisson ratio, and R is the grain radius.

For a dry medium composed of spheres, this readily yields the following one-dimensional EOS relation [16] in which the effective stress, σ_{eff} , is proportional to $\varepsilon^{3/2}$. As a result, the contact contribution to the sound speed, $c(\varepsilon) = (\rho^{-1}d\sigma_{\text{eff}}/d\varepsilon)^{1/2} \propto \sqrt{\varepsilon}$, where ρ is density, tends to zero at small positive strains. (Negative strain means that grains separate, and there are no contact forces present.) However, $dc/d\varepsilon$, which is a measure of nonlinearity, tends toward infinity! In real experiments, the aggregate is subject to a static pressure creating a constant pre-strain, ε_0 , and for small one-dimensional perturbations, we can expand σ into the series (2), where the modulus M is proportional to $\varepsilon_0^{1/2}$, and the quadratic and cubic nonlinearity coefficients are

$$\beta = 1/(2\varepsilon_0), \quad \delta = 1/(6\varepsilon_0^2). \quad (5)$$

In rock, the role of pre-strain can be played by a hard, consolidated fraction of contacts and/or by the pressure from upper layers of earth.

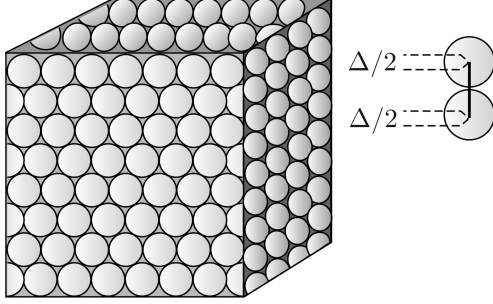


Fig. 9. An aggregate of contacting grains.

Some interesting properties of granular materials follow from these simple results. For instance, the nonlinearity parameters do not depend on grain size or on their composition, but on pre-strain ε_0 , i.e., on static pressure. These results were confirmed in experiments with lead shot and tuff excited at frequencies of a few kilohertz by a vibrating table [22]. The values of ε_0 were controlled by loading masses. From measurements of second and third harmonics, formulas (5) both gave good agreement with the experiment, whereas the parameter β exceeded 10^3 and δ exceeded values of $5 \cdot 10^6$.

Hence, this model predicts a very strong nonlinearity as compared with the solid matrix, and it admits many effective extensions. One of them deals with small-scale multicontact interfaces between larger grains, yielding a significant local amplification of nonlinearity from local stress concentrations. Estimates [17] show that for larger grains (of radius R) in contact with smaller hemispheres of radius r , the nonlinear portion of the EOS and, correspondingly, the nonlinearity parameters (5) acquire an additional term of $s(R/r)^{3/2}$, where s is the relative contact area occupied by small-sphere contacts (the remaining area is assumed to be cemented). This approach can be extended to more complicated fractal structures.

An interesting physical problem is associated with the effect of intergrain fluid. A 100% saturation decreases nonlinearity due to decreasing linear compressibility. However, a small amount of liquid can increase nonlinearity thanks to the effect of capillary forces or, for even thinner contacts of grains, to the Van der Waals force. The increase in nonlinearity at small and moderate fluid saturation has been confirmed experimentally [23]. This area is, however, beyond the scope of this paper.

The above effects are sufficient to provide extremely strong nonlinearity but still fail to include hysteresis. For the latter, transverse deformation can be important. In a series of papers by D. Johnson and colleagues (see [24] and references therein), a detailed analysis of nonlinear properties of granular media under the influence of static pressure was investigated. These authors took into account both the Hertz theory and the Mindlin relation (and its variations) stating that upon normal compression, a tangential displacement, τ , of contacting may arise that, in general, creates an additional transverse force:

$$\delta T = \frac{4\mu a(\Delta)\tau}{1-\nu}. \quad (6)$$

Here again, Δ is the relative displacement of spheres, μ is the shear modulus of the material, and a is a characteristic length depending on the nature of the surface contacts. For a “pure” Hertzian contact with reversible slip, $a = 0$, but for a rough, nonslip contact, it is equal to $\sqrt{R\Delta}$ or, in the case of pre-compression with an initial contact radius b , $a = [(R^2\Delta^2 + b^4/4)^{1/2} + b^2/2]^{1/2}$. This results in new features such as the dependence of forces and energy on the path of deformation. Indeed, in general, transposing of normal

and transverse displacements changes the work of external force. This is actually a hysteretic phenomenon that causes, for example, attenuation of an elliptically polarized acoustic wave. However, the role of this mechanism in rock hysteresis is still unclear, and below, we shall incorporate the description suggested several decades earlier for hysteretic behavior of metals.

3.2. Granato–Lücke model

In many hysteretic materials, the bond system is crystalline. Therefore, dislocations within the crystal lattice of the bond system could conceivably produce a nonlinear response. A physical model based on dislocations in metals was suggested by Granato and Lücke (G-L) as early as the fifties [25]. They used the analogy between a segment of a dislocation line pinned to impurity atoms and the motion of a string in order to describe elastic deformations (Fig. 10a). As the stress increases (normally shear stress), dislocations deform like pieces of string until, at some critical stress, they are disconnected from all impurity atoms between the nodes of a crystalline structure. As a result, the material becomes softer, which results in a strong nonlinearity of the stress–strain dependence (Fig. 10b, solid line). This process is irreversible: upon reducing stress, the system returns to equilibrium along a “soft” line. However, the resulting equilibrium state may be the same before and after inducing the dislocations to react, so that we have a type 1 hysteresis. The model also incorporates slow dynamics because the equilibrium state takes some time to restore. In reality, the distances between the sticking points are statistically distributed, which smooths the hysteretic loop (Fig. 10b, dashed line). Hybrids of the G-L model include other aspects including frequency dependence. In spite of some disadvantages, this model was truly a pioneering micromodel for the hysteretic dynamic behavior of structurally inhomogeneous materials.

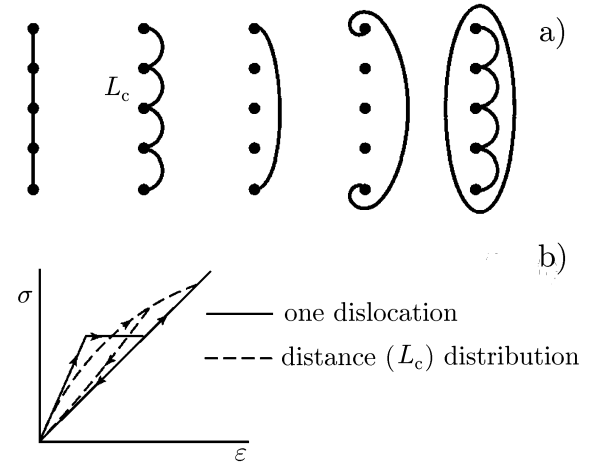


Fig. 10. Granato–Lücke model of dislocations (a). Resulting stress–strain curve for a single dislocation (solid line) and a distribution of dislocations (dashed line) (b).

4. NONLINEAR OSCILLATIONS AND WAVES IN ROCKS

In order to explain the experimental data, it is necessary, along with construction of material models, to understand the peculiarities of waves in these materials. From the above considerations and experimental data, it can be expected that these processes are more complex than those in nonlinear acoustics describing most fluids and intact solids.

4.1. Classical theory

The equation of motion in Lagrangian coordinates is

$$\rho \ddot{u}_i = \frac{\partial \sigma_{ij}}{\partial x_j}, \quad (7)$$

where u_i are the components of the displacement vector, \mathbf{u} ; and ρ , σ_{ij} , and $\ddot{\mathbf{u}}$ designate the density, the stress tensor, and the particle acceleration, respectively.

To gain an insight, one can consider the one-dimensional case. For a longitudinal wave (P -wave) propagating in an isotropic medium, a one-dimensional wave can exist with only nonzero components $\sigma_{xx} = \sigma$

and $u_x = u$ or $\varepsilon_{xx} = \varepsilon = \partial u / \partial x$. The resulting equation of motion can be written as

$$\rho_0 \frac{\partial^2 \varepsilon}{\partial t^2} = \frac{\partial^2 \sigma(\varepsilon)}{\partial x^2}. \quad (8)$$

From the energy expansion, the EOS can be written as (2). Correspondingly, the local sound velocity is

$$c = \sqrt{\rho^{-1} d\sigma/d\varepsilon} \approx c_0(1 + 2\beta\varepsilon + \delta\varepsilon^2 + \dots), \quad (9)$$

with $c_0 = \sqrt{M/\rho}$.

Note that even if the nonlinearity is anomalously large in rocks in comparison with that of atomic elastic media, the nonlinear terms in the EOS are generally much smaller than the linear term. This is because ε is of the order of $10^{-9} - 10^{-5}$ in dynamic experiments. Therefore, one can use the relation (8) and its generalizations for media with strong nonlinearity.

This nonlinearity can be caused by two mechanisms. The first is of a “geometrical” or “kinematic” type, associated with the difference between the Lagrangian and Eulerian descriptions of motion (such as $(\mathbf{u}\nabla)\mathbf{u}$ in the Eulerian equation of motion). The other type is “physical” elastic nonlinearity. Physical nonlinearity is described by third-order (and higher) terms in the expansion of the elastic energy in ε , and accounts for the fact that stress is not a linear function of strain. Geometrical nonlinearity is typically comparable in order to physical nonlinearity in atomic elastic materials, such as fluids and intact solids. In rock and other highly nonlinear media, physical nonlinear response is typically orders of magnitude larger than geometric nonlinear response, and therefore, the latter (and hence the difference between Eulerian and Lagrangian descriptions) can be ignored, which somewhat simplifies the mathematics.

4.2. Traveling waves and hysteresis

For hysteretic media, we begin by considering traveling (progressive) waves in an unbounded material. For a one-dimensional traveling wave, the strain $\varepsilon \approx -v/c$, where $v = u_t$ is the particle velocity, and c is sound velocity. In this case, ε plays the role of the acoustic Mach number. When the Taylor expansion (9) for c is valid, a well-known solution in the form of a simple (Riemann) wave follows from Eq. (8):

$$\varepsilon = \mathcal{F}[x - c(\varepsilon)t], \quad (10)$$

where \mathcal{F} is an arbitrary function defined by the initial condition, and $c(\varepsilon)$ is the local wave speed. Propagation of such a wave in acoustics is known to result in the appearance of shocks and then the formation of a sawtooth wave (e.g., [18]), which dissipates asymptotically as t^{-1} at a sinusoidal initial condition.

Looking back at the experiments, we see nonclassical, hysteretic behavior of rock and turn to wave solutions that can describe this behavior. The evolution of a nonlinear wave in hysteretic media described by Eq. (3) is considerably different from that of a wave in classical nonlinear media. Several problems of this kind have already been addressed in publications (e.g., [26–29]). Here we give only a few simple illustrations. Available phenomenological models of hysteretic stress–strain dependence can include rather many parameters, and the choice should be based on experimental results. We mention here both basic hysteretic models outlined above, of types 1 and 2 (Figs. 8a and 8b), for which the wave distortion processes are significantly different from each other and from the classical case. Here, we restrict ourselves by symmetric hysteretic loops. Thus, for type 1

$$\sigma = \begin{cases} (E - \alpha\varepsilon_m)\varepsilon + (\gamma/2)(\varepsilon_m^2 - \varepsilon^2), & \dot{\varepsilon} > 0; \\ (E - \alpha\varepsilon_m)\varepsilon - (\gamma/2)(\varepsilon_m^2 - \varepsilon^2), & \dot{\varepsilon} < 0, \end{cases} \quad (11)$$

where E is the linear elasticity modulus, ε_m is maximal strain corresponding to the singular points of EOS, and γ is the nonlinearity parameter; for weak nonlinearity, $\gamma\varepsilon_m \ll 1$. This relationship corresponds to an irreversible hysteresis in the sense that $\varepsilon \neq 0$ for $\sigma = 0$ and vice versa. If the process starts from zero, it first goes along some path up to the singular point $\varepsilon = \varepsilon_m$, and then continues periodically along the loop (11).

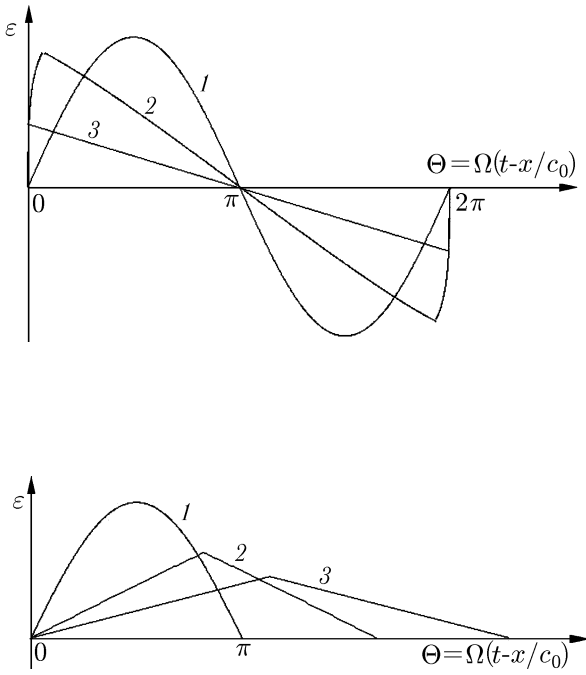


Fig. 11. Qualitative evolution of the wave profile as a function of the “traveling phase” $\Theta = \Omega(t - x/c_0)$ in a nonhysteretic medium with a quadratic nonlinearity (a), in a type 1 hysteretic model (b), and in a type 2 hysteretic model (c). Curves 1, 2, and 3 correspond to three successive points along the propagation path. For (a) and (b) the input wave is sinusoidal with frequency Ω , for (c) it is a unipolar pulse in the form of a half-period of a sinusoid with the frequency Ω .

The type 2 model is described by the equation

$$\sigma(\varepsilon, \dot{\varepsilon}) = E \begin{cases} \varepsilon - \gamma\varepsilon^2/2, & \text{if } \varepsilon > 0 \text{ and } \dot{\varepsilon} > 0; \\ \varepsilon + \gamma\varepsilon^2/2 - \gamma\varepsilon_m\varepsilon, & \text{if } \varepsilon > 0 \text{ and } \dot{\varepsilon} < 0; \\ \varepsilon + \gamma\varepsilon^2/2, & \text{if } \varepsilon < 0 \text{ and } \dot{\varepsilon} < 0; \\ \varepsilon - \gamma\varepsilon^2/2 + \gamma\varepsilon_m\varepsilon, & \text{if } \varepsilon < 0 \text{ and } \dot{\varepsilon} > 0. \end{cases} \quad (12)$$

In this case, the loops beginning from zero are reversible.

Let us now describe traveling waves within the framework of these two EOS. As long as nonlinearity is small, each piece of a wave corresponding to a given branch of hysteretic EOS propagates as a simple wave (10) without reflections. They should be matched at $\varepsilon = \varepsilon_m$. Some analytical expressions for the wave (10) can be found, for example, in [29]. They are rather cumbersome due to the dependence of the wave amplitude ε_m on time. Qualitative pictures of nonlinear wave evolution for different cases are shown in Fig. 11. Figure 11a demonstrates a classical case: the evolution of an initially sinusoidal wave in a nonhysteretic medium with quadratic nonlinearity. In this case, a sawtooth wave is eventually formed. Due to hysteresis, an additional kind of singularity arises. In general, due to singularity at the wave maximum, the portions on either side of the wave peak move with different velocities, thus “consuming” each other and resulting in the formation of a cusp. Figure 11b shows such a process for the type 1 EOS and Fig. 11c, for the type 2 EOS. In the latter case, a unipolar pulse is shown; otherwise, additional singularities in the zero point may occur.

The corresponding asymptotic behavior of wave amplitude at large distances is also different. For example, for the type 1 hysteresis (11), the wave amplitude ε_m changes as $1/t$, as in a classical periodic sawtooth wave. Needless to say, the wave profiles are radically different from their classical “prototypes.” Correspondingly, whereas all harmonics are represented in the classical sawtooth wave, only odd harmonics exist in the symmetric hysteretic case.

In short, the presence of hysteresis qualitatively changes the wave profile evolution in comparison with the classical case.

4.3. Resonance oscillations

The theory for nonlinear standing waves is more complicated due to nonlinear interactions of oppositely propagating waves. In the general case, one should solve a nonlinear wave equation (8) with an external forcing and boundary conditions at the end of the bar. In terms of displacement u , this equation is

$$\rho \left(\ddot{u} + \frac{\omega}{Q} \dot{u} \right) = \frac{\partial \sigma}{\partial x} + \frac{1}{2} F_0(x) \left[e^{i(\omega + \Delta)t} + \text{c.c.} \right], \quad (13)$$

where $F_0(x)$ is the external force amplitude, Q is the linear quality factor, Δ is the frequency shift (detuning) from a linear resonance mode, and c.c. denotes complex conjugate.

For a small nonlinearity, the structure of resonance modes is close to that of the linear system, although their amplitudes are strongly affected by nonlinear interaction. Thus, it is adequate to use an expansion of the solution for u into the modal series:

$$u = \sum_n A_n(t) \Phi_n(x), \quad (14)$$

where Φ is the eigenfunction of the linear wave to be found with the use of corresponding boundary conditions at the bar ends (for a bar of length L with free ends, $\Phi_n = \cos(kx)$, where $k = n\pi/L$ and n is an integer mode number). As a result, we obtain a system of ordinary differential equations for A_n that can usually be reduced to a system of a few interacting resonant modes (e.g., [30]).

Substituting a solution in the form (14) for the n th mode, e.g., $u = U \cos(k_n x) \exp[-i(\omega_n + \Delta)t/2]$, into Eq. (13), multiplying by $\cos(k_n x)$ and integrating over the length L of the bar, we obtain the following equation for the amplitude U in equilibrium:

$$-\rho (\omega_n U \Delta + i\omega_n^2/(2Q)) = k_n \langle \sigma_1^N \rangle + \langle F_{0n} \rangle. \quad (15)$$

The stress is $\sigma = E(\varepsilon) + \sigma^N(\varepsilon)$ with N denoting the small nonlinear portion, σ_1^N is the amplitude of the first temporal harmonic of the nonlinear part of the stress, and E is the linear modulus, so that $c_0 = \omega_n/k_n = (E/\rho)^{1/2}$. Here Q is the linear quality factor, and $\langle \sigma_1^N \rangle = L^{-1} \int_0^L \sigma_1^N(x) \cos(k_n x) dx$ denotes spatial averaging. Hence, we have an equation for the amplitude-frequency resonance dependence. In terms of strain $\varepsilon = \partial u/\partial x$, the result is

$$\varepsilon_m = \frac{\varepsilon_0}{L \sqrt{((\Delta + \Delta^N)/c_0)^2 + (k_n/2Q_N)^2}}, \quad (16)$$

where $Q_N < Q$ is the quality factor taking into account both linear and nonlinear losses and Δ^N is the nonlinear frequency shift. Nonlinear losses and frequency shift depend on the imaginary and real parts of $\langle \sigma_1^N \rangle$. Here, it is supposed that the excitation occurs in a fixed point $x = 0$, i.e., $u(0, t) = u_0 \sin(\omega t)$, and $\varepsilon_0 = k_1 u_0$.

The result clearly depends on the EOS of the medium. In a classical ‘‘cubic’’ medium, where $\sigma^N \propto \varepsilon^3$, this relation defines a well-known nonlinear resonance curve corresponding to the known Duffing oscillator, with the nonlinear frequency shift proportional to ε_0^2 . In hysteretic media considered above, the wave profile is distorted according to the above consideration of traveling waves. Note that, unlike in classical media, the Taylor expansion of $\langle \sigma_1^N \rangle$ contains not only odd but also even powers of ε . As a result the third harmonic in hysteretic media can be proportional to ε^2 as observed.

For strong wave distortion, a relatively simple way to treat the problem is to consider a ring resonator [17] (similar to that used in experiments described in [30]) where a resonance mode can be a wave traveling around the ring and undergoing nonlinear distortion until it is balanced with a harmonic source applied at some point. Hysteretic media described by the two aforementioned types of phenomenological stress–strain loops yield different results.

Let us denote by $\nu(\varepsilon_1)$ the relative change of the amplitude of the fundamental harmonic ε_1 of the wave upon propagation at the distance of the bar length, and suppose that $g \ll 1$. The wave excited at $x = 0$ has the form $u(0, t) = u_0 \sin(\omega t)$, so that the first harmonic arriving at $x = 0$ after passing the ring length L will have the delay of L/c and decay by a factor of g , which in the steady-state regime is to be compensated for by the source. Thus, the balance equation for ε_1 takes the form

$$\varepsilon_1 - \varepsilon_1 \left[1 - \nu(\varepsilon_1) \right] e^{-ikL} = ku_0. \quad (17)$$

The solution of this equation can be represented as Eq. (16) plus the expression for $\langle \sigma_1^N(\varepsilon_m) \rangle$ depending on the EOS model. For illustration, we suppose that the excitation amplitude is large enough and, consequently, a steady-state travelling nonlinear wave excited in the ring has an asymptotic form with cusps corresponding to Figs. 11a and 11b. Briefly, the results are the following.

In both cases, the nonlinear Q -factor for the n th mode is given by

$$Q_N^{-1} = \frac{\omega_n}{2\pi c_0} g \varepsilon_1, \quad (18)$$

where $g = 2\pi^2\gamma$ for the type 1 model (11) and $g = 4\pi^2\gamma$ for the type 2 model (12).

The nonlinear resonance frequency shift is

$$\delta\omega_n = -\frac{\pi\omega_n\varepsilon_1\beta}{2c_0}, \quad (19)$$

with $\beta = \gamma$ for type 1 hysteresis and $\beta = \alpha$ for type 2 one. Hence, both the losses and the frequency shift are proportional to the amplitude of excited oscillations, and the resonance curves look as in Fig. 2b. However, the relation between ε_1 and the input strain ε_0 in resonance depends itself on the nonlinear losses and, as a result, on the EOS.

Similarly, a higher m th harmonic of oscillations at a given mode can be considered by using the perturbation method (small harmonic amplitudes) and the corresponding stress harmonic amplitude, $\langle \sigma_m^N \rangle$. For hysteretic models with singularities, we obtain different dependences which are often observed in experiments with rocks.

5. CONCLUSIONS

Oscillations and waves in hysteretic media may appear an arcane subject. At the same time, as illustrated above, in the dynamics of rocks, some ceramics, some metals, and damaged materials, hysteresis is a rule rather than an exception. This is seen from the experimental results outlined above: the micro-to-nanoscale “bond system” (microcracks, dislocations, etc.) responsible for strong hysteretic nonlinearity. Such “violations” are so ubiquitous that a regular crystalline structure can be considered almost as an exception for macroscopic solids found in nature. This is an extremely rich area of material physics which can be considered as a bridge between the macroscopic mechanical properties, mesoscopic granular structure, and nanoscale features that appear responsible for the hysteretic behavior. A joint mechanical, thermodynamical, and possibly even quantum-physics approach may be necessary for understanding the physics of nonlinearity in rocks. In addition, the practical significance of nonlinear methods of non-destructive evaluation of materials (e.g., [31]) has been already demonstrated. At the same time, it opens an interesting chapter in nonlinear wave theory which deserves to be more actively addressed.

REFERENCES

1. A. Andronov, A. Vitt, and S. Khaikin, *Theory of Oscillations*, Dover, New York (1987).
2. A. Gaponov L. Ostrovsky, and G. Freidman, *Sov. Radiophysics* (1967).

3. R. Guyer and P. Johnson, *Physics Today*, **52**, 30 (1999).
4. L. Ostrovsky and P. Johnson, *Riv. Nuovo Cimento* (2001), in press.
5. L. Hilbert, T. Hwong, N. Cook, K. Nihei, and L. Myer, in: P. P. Nelson and S. E. Laubach (eds.), *Rock Mechanics Models and Measurements Challenges from Industry*, A. A. Balkema, Rotterdam (1994), p. 497.
6. J. Jaeger and N. Cook, in: *Fundamentals of Rock Mechanics*, 3rd Edition, Chapman and Hall, London (1979), p. 78.
7. R. Guyer, K. McCall, G. Boitnott, L. Hilbert, and T. Plona, *J. Geophys. Res.*, **102**, 5281 (1997).
8. P. Johnson, B. Zinszner, and P. Rasolofosaon, *J. Geophys. Res.*, **101(B5)** (1996)
9. V. Nazarov, L. Ostrovsky, I. Soustova, and A. Sutin, *Phys. Earth Planet. Interiors*, **50**, 65 (1988).
10. J. Tencate and T. Shankland, *Geophys. Res. Lett.*, **23**, 3019 (1996).
11. J. Tencate, J. Smith, and R. Guyer, *Phys. Rev. Lett.*, **85**, 1020 (2000).
12. K. Ishihara, *Soil Behaviour in Earthquake Geotechnics*, Clarendon Press, Oxford (1996).
13. V. Nazarov, L. Ostrovsky, I. Soustova, and A. Sutin, *Acoust. Phys.*, **30**, No. 5, 827 (1994).
14. S. V. Zimenkov and V. Nazarov, *Izv., Fiz. Zemli*, **29**, 12 (1994).
15. R. Guyer, P. Johnson, and J. Tencate, *Phys. Rev. Lett.*, **82**, 3280 (1999).
16. I. Belyaeva, L. Ostrovsky, and V. Zaitsev, *Nonlinear Processes in Geophysics*, **4**, 1 (1997).
17. L. Ostrovsky, P. Johnson, and T. Shankland, in: W. Lauterborn and T. Kurz (eds.), *Nonlinear Acoustics at the Turn of the Millennium, ISNA 15, Göttingen, 1999*, Amer. Inst. of Physics, Melville, N.Y., (2000), pp. 75–84.
18. K. A. Naugolnykh and L. A. Ostrovsky, *Nonlinear Wave Processes in Acoustics*, Cambridge Univ. Press, Cambridge–New York (1998).
19. L. Landau and E. Lifshits, *Theory of Elasticity, 3rd edition*, Pergamon Press, Oxford (1986).
20. S. Asano, *J. Phys. Soc. Japan*, **29**, 952 (1970).
21. R. Guyer, K. McCall, G. Boitnott, L. Hilbert, and T. Plona, *J. Geophys. Res.*, **102** 5281 (1995).
22. I. Belyaeva, L. Ostrovsky, and E. Timanin, *Acoust. Lett.*, **15(11)**, 221 (1992).
23. K. Van den Abeele, J. Carmeliet, P. Johnson, and B. Zinszner, *J. Geophys. Res.*, (2000), submitted.
24. D. Johnson, H. Makse, N. Gland, and L. Schwartz, *Physica B*, **279**, 134 (2000).
25. A. Granato and K. Lücke, *J. Appl. Phys.*, **27** 583 (1956).
26. V. Nazarov, *Acoust. Phys.*, **43**, 192 (1997).
27. K. Van den Abeele, P. Johnson, R. Guyer, and K. McCall, *J. Acoust. Soc. Am.*, **101(4)** 1885 (1997).
28. V. Gusev, C. Glorieux, W. Lauriks, and J. Thoen, *Phys. Lett. A*, **232** 77 (1997).
29. V. Gusev, *J. Acoust. Soc. Am.*, **107(6)**, 3047 (2000).
30. L. Ostrovsky, I. Soustova, and A. Sutin, *Acustica*, **5**, 298 (1978).
31. K. Van den Abeele, P. Johnson, AND A. Sutin, *Research on Nondestructive Evaluation*, **12/1**, 17 (2000).